

## Research Article

# Performance of Pt–Ru–Ni/MC ternary electrocatalyst on methanol oxidation reaction in membraneless fuel cells

P. Ramar<sup>1</sup>, M. Chitrlekha<sup>2,\*</sup>

<sup>1</sup>Department of Chemistry, Government Arts College, Ariyalur - 621 713, India.

<sup>2</sup>Department of Chemistry, D G Government Arts College, Mayiladuthurai, India.

\*Corresponding author's e-mail: [chitrlekha2@yahoo.com](mailto:chitrlekha2@yahoo.com)

### Abstract

In the present work, mesoporous carbon (MC) supported Pt–Ni, Pt–Ru, and Pt–Ru–Ni electrocatalysts with different atomic ratios were synthesized by NaBH<sub>4</sub> reduction method to study the electro-oxidation of methanol in a MLMFC. The synthesized electrocatalysts were characterized by TEM, EDX and XRD analyses. The Pt metal was the predominant material in all the samples, with peaks attributed to the face-centered cubic (fcc) crystalline structure. The TEM analysis indicated that the prepared catalysts had similar particle morphology, and their particle sizes were 3–5 nm. The electrocatalytic activities of the synthesized electrocatalysts were characterized by cyclic voltammetry (CV) and chronoamperometry (CA). During the experiments performed on single membraneless fuel cells, Pt50Ru40Ni10/MC performed better among all the catalysts prepared with power density of 38.1 mW cm<sup>-2</sup>. The enhanced methanol oxidation activity by Ni in Pt50Ru40Ni10/MC can be attributed to the electronic effect as the result of the modification of electronic properties of Pt and the various oxidation states of Ni. In our work, for the first-time mesoporous carbon-supported binary Pt–Ru, Pt–Ni and ternary Pt–Ru–Ni anode catalysts were successfully tested in a single membraneless fuel cell using 1.0 M methanol as the fuel and 0.1 M sodium percarbonate as the oxidant in the presence of 0.5 M H<sub>2</sub>SO<sub>4</sub> as the electrolyte at room temperature.

**Keywords:** Mesoporous carbon; Platinum; Nickel; Ruthenium; Methanol; Catalysts.

### Introduction

The membraneless methanol fuel cell (MLMFC) is an efficient electrical power source when using methanol as the fuel. However, the CO poisoning of Pt anode limited the potential use of methanol fuel cells for vehicular applications. Therefore, alloying of platinum with other metals such as Ru, Pd, Mo, Sn, Co, Cu, W and Ni have been studied as a convenient method of modifying the electrocatalytic properties of platinum in order to reduce or avoid the poisoning effect [1-3]. Among all the catalyst systems, Pt–Sn/MC and Pt–Ru/MC catalysts have received more attention due to its high CO tolerance, which can be achieved via its electronic effects and bifunctional mechanisms that improve the catalytic activities of electrochemical reactions [4-5]. However, comparing the electrocatalytic activity of Pt–Sn/MC and Pt–Ru/MC catalysts, Pt–Sn/MC electrocatalyst has been more active than the Pt–Ru/MC electrocatalyst for methanol

and ethanol oxidation at room temperature. Nevertheless, efforts are being made to improve the performance of Pt–Ru/MC anode catalysts for methanol oxidation to a suitable level for commercialization.

The performance of Pt–Ru/MC electrocatalysts also depends on the preparation procedures and their atomic ratios. Neto et al. investigated the electro-oxidation of methanol and ethanol with Pt–Ru ternary alloy catalysts prepared via an alcohol-reduction process using ethylene glycol as the solvent and a reduction agent [6]. Recently, Chen et al. prepared a Pt–Ru ternary alloy by the sodium borohydride (NaBH<sub>4</sub>)-reduction method to compare the study of tungsten-modified Pt–Ru electrocatalysts for methanol oxidation [7]. Despite the controversies, recent studies have shown that the addition of Ni to Pt and Pt–Ru catalysts can enhance electrocatalytic activity for methanol oxidation. For example, Wang et al. prepared PtRuNi/C electrocatalysts by reduction with

NaBH<sub>4</sub> for methanol oxidation [8]. Jeon et al. also observed that PtRuNi/C electrocatalyst prepared by NaBH<sub>4</sub> reduction was more active for methanol oxidation than a commercial PtRu/C electrocatalyst. And, more recently, Ribeiro et al. prepared PtRuNi/C electrocatalysts by an alcohol-reduction process for electro-oxidation of methanol [9]. In the present work Pt50Ni50/MC and Pt50Ru50/MC and Pt50Ru40Ni10/MC catalysts were prepared by sodium borohydride reduction method. The prepared catalysts are characterized using X-ray diffraction analysis, energy dispersive X-ray (EDAX), and transmission electron microscope (TEM). Methanol electro-oxidation in the presence of the above prepared catalysts is studied using cyclic voltammetry (CV), and chronoamperometry (CA). Finally, the catalysts are tested as anode in the MLMFC.

## Experimental

### Materials

The metal precursors used for the preparation of electrocatalysts were H<sub>2</sub>PtCl<sub>6</sub>·6H<sub>2</sub>O (from Sigma Aldrich), RuCl<sub>3</sub>·3H<sub>2</sub>O (from Sigma Aldrich) and NiCl<sub>2</sub>·6H<sub>2</sub>O (from Sigma Aldrich). Mesoporous carbon (from Cabot Corp.) was used as a support for the catalysts. Graphite plates (3 cm long and 0.1 cm wide from E-TEK) were used as substrates for the catalyst to prepare the electrodes. Nafion® (DE 521, DuPont USA) dispersion was used to make the catalyst slurry. Isopropyl alcohol (from Merck) was used as a solvent and NaBH<sub>4</sub> (from Merck) was used as the reduction agent. Methanol (from Merck), sodium percarbonate (from Riedel) and H<sub>2</sub>SO<sub>4</sub> (from Merck) were used as the fuel, the oxidant and as the electrolyte for electrochemical analysis, respectively. All the chemicals were of analytical grade. Pt/MC (40-wt%, from E-TEK) was used as the cathode catalyst.

### Catalyst Preparation

Mesoporous carbon supported ternary Pt–Ru–Ni catalysts with different atomic ratios were synthesized by using a conventional reduction method with NaBH<sub>4</sub> [10]. The mesoporous carbon was ultrasonically dispersed in a mixture of ultrapure water (Millipore MilliQ, 18 MΩ cm), and isopropyl alcohol for 20 min. The precursors were added to the ink and then mixed thoroughly for 15 min. The pH value of the ink was adjusted by NaOH solution to 8 and then

raised its temperature to 80 °C. Twenty-five milliliters of 0.2 mol L<sup>-1</sup> solution of sodium borohydride was added into the ink drop by drop, and the bath was stirred for 1 h. The mixture was cooled, dried and washed repeatedly with deionized (DI) water until no Cl<sup>-</sup> ions existed. The catalyst powder was dried for 3 h at 120 °C and stored in a vacuum vessel. For comparison, the monometallic Pt/MC, bimetallic Pt–Ru/MC and Pt–Ni/MC catalysts were synthesized under the same conditions. The electrocatalytic mixtures and atomic ratios were Pt50Ru40Ni10/MC, Pt50Ru50/MC, Pt50Ni50/MC, and Pt100/MC. The nominal loading of metals in the electrocatalysts was 20 %wt. and rest 80 %wt. was mesoporous carbon.

## Results and discussions

### Physical Characterization

#### X-ray diffraction (XRD)

The XRD patterns of the prepared Pt50Ru40Ni10/MC, Pt50Ru50/MC, Pt50Ni50/MC and Pt100/MC catalysts are shown in Fig. 1. The first peak located at around 25° in all the XRD patterns is attributable to the mesoporous carbon support. The other peaks are the characteristics of face-centered-cubic (fcc) crystalline Pt at 2θ values of 39°, 47°, 67° and 82° and are indexed with planes (1 1 1), (2 0 0), (2 2 0) and (3 1 1), respectively. No diffraction peaks were attributed to pure ruthenium and nickel or their oxides/hydroxides in XRD patterns, suggesting that ruthenium and nickel atoms either form an alloy with platinum or exist as amorphous oxide phases [11–13]. The Pt–Ni/MC electrocatalyst also showed the same characteristic peak as that of the Pt–Ru/MC electrocatalysts.

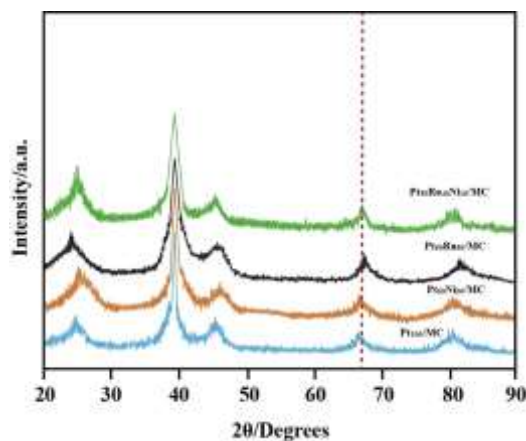


Fig. 1. X-ray diffraction patterns of Pt50Ru40Ni10/MC, Pt50Ru50/MC, Pt50Ni50/MC and Pt100/MC catalysts

The fcc lattice parameters were evaluated from the angular position of the (2 2 0) peaks, which reflect the formation of a solid solution. The lattice parameters obtained for the Pt–Ni/MC (0.3904), Pt–Ru/MC (0.3887 nm) and Pt–Ru–Ni/MC (0.3898 nm) catalysts are smaller than those for Pt/MC electrocatalyst (0.3915 nm). It indicates that, the decrease in lattice parameters of the alloy catalysts reflects the progressive increase in the incorporation of Ru and Ni into the alloyed state. The difference of lattice parameters and the shift of (2 2 0) plane indicate interactions between Pt, Ru and Ni. The average particle size for Pt–Ru/MC, Pt–Ni/MC, and Pt–Ru–Ni/MC electrocatalysts were in the range of 3–5 nm was estimated using the Scherrer equation (Table 1).

### Transmission Electron Microscopy (TEM)

TEM image of the Pt<sub>50</sub>Ru<sub>40</sub>Ni<sub>10</sub>/MC alloy catalyst and the corresponding particle size distribution histogram based on the observation of more than 500 nanoparticles are presented in Fig. 2. The Pt<sub>50</sub>Ru<sub>40</sub>Ni<sub>10</sub>/MC alloy nanoparticles are well dispersed on the surface of the support with a very narrow size distribution. The obtained mean particle diameter is about 3–5 nm, which is in fairly good agreement with the data calculated from XRD. In comparison to Pt<sub>50</sub>Ru<sub>40</sub>Ni<sub>10</sub>/MC the mean particle size of Pt<sub>50</sub>Ru<sub>50</sub>/MC is only slightly smaller. The particle size distribution of these catalysts is shown in Table 1 in accordance to the TEM images.

Table 1. The EDX composition, lattice parameters, and the particle size obtained for different atomic ratios of electrocatalysts

Electrocatalyst	Nominal Atomic ratio			EDX Atomic ratio			Lattice parameter (nm)	Crystallite size (nm)	Particle size from TEM (nm)
	Pt	Ru	Ni	Pt	Ru	Ni			
Pt/MC	100	-	-	99	-	-	0.3915	5.5	5.1
Pt–Ni/MC	50	-	50	51	-	49	0.3904	4.2	4.1
Pt–Ru/MC	50	50	-	52	48	-	0.3887	3.7	3.4
Pt–Ru–Ni/MC	50	40	10	52	39	9	0.3898	3.3	3.2

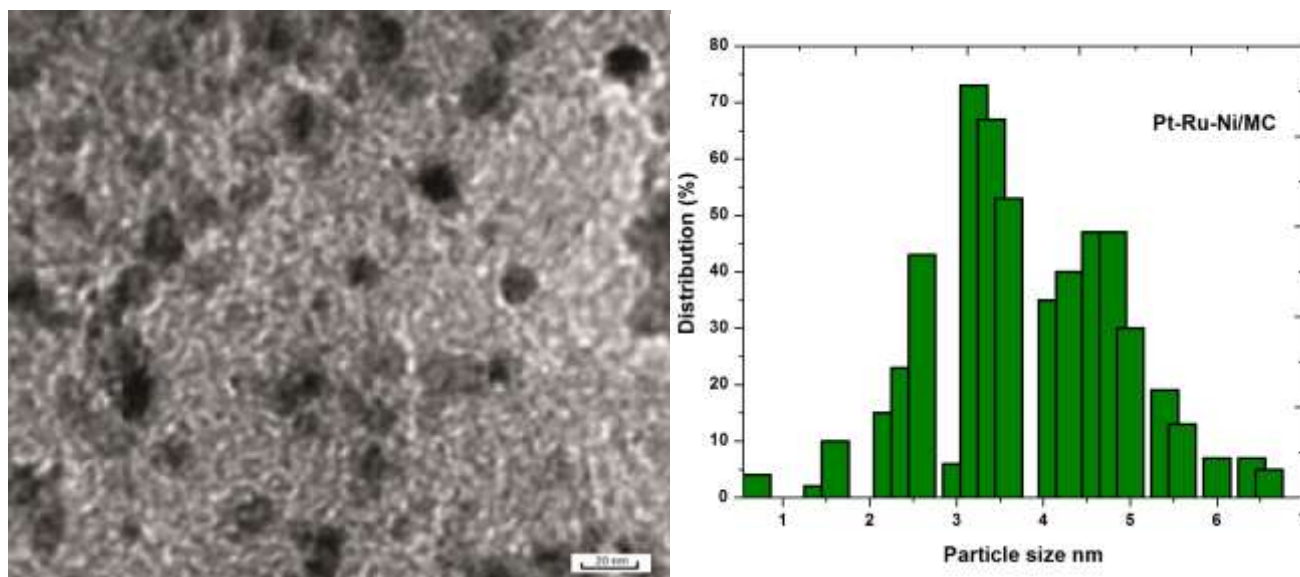


Fig. 2. TEM image and particle size distribution of Pt<sub>50</sub>Ru<sub>40</sub>Ni<sub>10</sub>/MC catalyst

### Energy Dispersive X-ray Spectroscopy (EDX)

Energy dispersive X-ray spectroscopy is conducted by focusing the electron beam on several different selected regions of the mesoporous carbon supported Pt–Ru–Ni nanoparticles. An EDX spectrum of Pt–Ru–Ni/MC nanoparticle is shown in Fig. 3. The average composition of the sample was in atom

ratio of Pt:Ru:Ni = 5:4:1. The compositions of Pt, Ru and Ni in different regions are in close agreement and have no significant deviations. The EDX results of the binary Pt–Ru/MC and Pt–Ni/MC and the ternary Pt–Ru–Ni/MC catalysts are very close to the nominal values, which indicate that the metals were loaded onto the mesoporous carbon support without obvious loss.

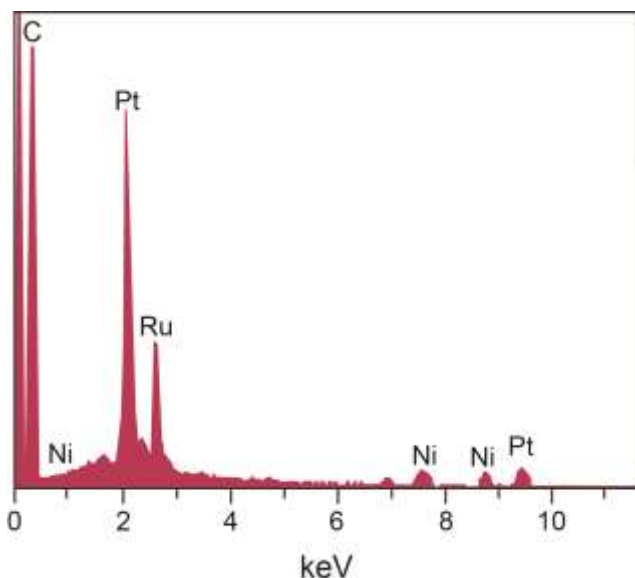


Fig. 3. EDX spectra of Pt–Ru–Ni/MC catalysts

### Electrochemical Characterization

#### Cyclic Voltammetry

Typical cyclic voltammograms (CVs) of Pt<sub>50</sub>Ru<sub>40</sub>Ni<sub>10</sub>/MC, Pt<sub>50</sub>Ru<sub>50</sub>/MC, Pt<sub>50</sub>Ni<sub>50</sub>/MC and Pt<sub>100</sub>/MC catalysts in 0.5 M H<sub>2</sub>SO<sub>4</sub> solution are shown in Fig. 4a. The CV curves were obtained in a half cell at a scan rate of 50 mV s<sup>-1</sup> between -0.1 and +1.0 V (vs. Ag/AgCl) in the absence of methanol and at room temperature. The characteristic features of polycrystalline Pt, i.e. hydrogen adsorption/desorption peaks in low potential region, oxide formation/stripping wave/peak in high potential region and a flat double layer in between, are observed for all the synthesized catalysts. The voltammograms of the electrocatalysts did not display a well-defined hydrogen region between 0.0 and 0.4 V, as the catalyst's features in this region are influenced by their surface composition. Taking the Pt<sub>100</sub>/MC composition as a reference, the binary Pt<sub>50</sub>Ru<sub>50</sub>/MC and Pt<sub>50</sub>Ni<sub>50</sub>/MC catalysts showed a voltammetric charge similar to that of the pure Pt catalyst. However, a considerable increase in the voltammetric charge of ternary Pt<sub>50</sub>Ru<sub>40</sub>Ni<sub>10</sub>/MC catalyst was observed in the double-layer region between 0.4 and 0.8 V, indicating that the addition of Ni into binary Pt–Ru/MC leads to an enhanced activity for the oxidation reactions. This behavior can be explained by a better material dispersion on carbon and the formation of ultrafine particles [14]. The latter phenomenon was being confirmed by XRD data, which give a *D* value close to 3 nm.

Fig. 4b corresponds to representative CVs of methanol oxidation under acidic conditions

(1.0 M CH<sub>3</sub>OH and 0.5 M H<sub>2</sub>SO<sub>4</sub>) catalyzed by Pt<sub>50</sub>Ru<sub>40</sub>Ni<sub>10</sub>/MC, Pt<sub>50</sub>Ru<sub>50</sub>/MC, Pt<sub>50</sub>Ni<sub>50</sub>/MC and Pt<sub>100</sub>/MC catalysts. For assessing the electrocatalytic activity of the working electrode, cyclic voltammetry was obtained in 1.0 M methanol and 0.5 M sulfuric acid solution with a scan rate of 50 mV s<sup>-1</sup>.

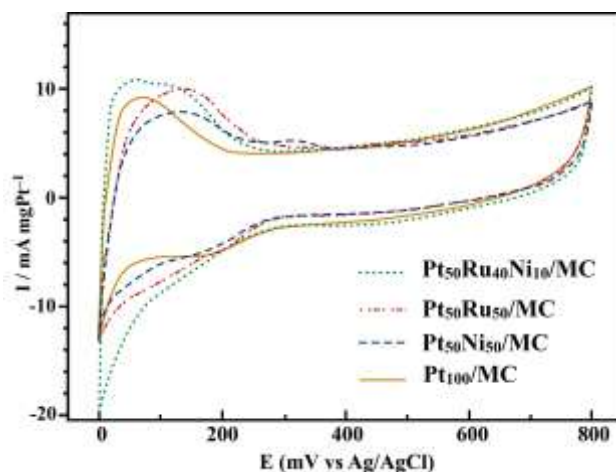


Fig. 4a. CVs Pt<sub>50</sub>Ru<sub>40</sub>Ni<sub>10</sub>/MC, Pt<sub>50</sub>Ru<sub>50</sub>/MC, Pt<sub>50</sub>Ni<sub>50</sub>/MC and Pt<sub>100</sub>/MC electrocatalysts at a scan rate of 50 mV s<sup>-1</sup> in 0.5 M H<sub>2</sub>SO<sub>4</sub> solution at room temperature

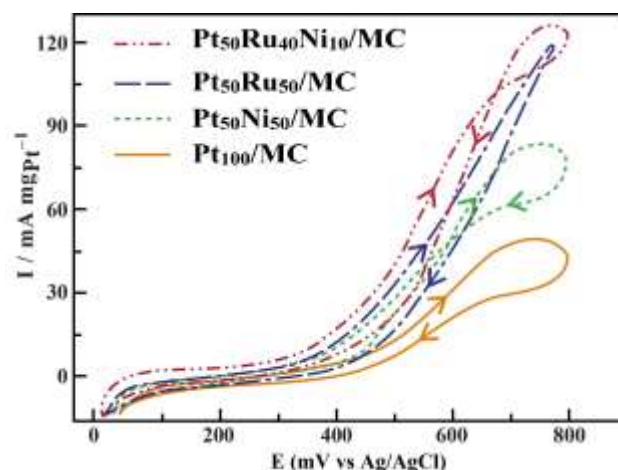


Fig. 4b. Cyclic voltammetry of Pt<sub>50</sub>Ru<sub>40</sub>Ni<sub>10</sub>/MC, Pt<sub>50</sub>Ru<sub>50</sub>/MC, Pt<sub>50</sub>Ni<sub>50</sub>/MC and Pt<sub>100</sub>/MC electrocatalysts in 1.0 M methanol+0.5 M H<sub>2</sub>SO<sub>4</sub> at room temperature with a scan rate of 50 mV s<sup>-1</sup>

All the current values were normalized by the geometric surface area of the electrode used. The CV curves depict the presence of a peak in the potential range of the positive sweep and another peak in the negative sweep. The peak in the positive sweep is associated with the methanol oxidation, and the peak in the negative sweep is related to the oxidation of carbonaceous intermediate products from incomplete methanol oxidation. The peak current densities of Pt<sub>50</sub>Ru<sub>40</sub>Ni<sub>10</sub>/MC, Pt<sub>50</sub>Ru<sub>50</sub>/MC, Pt<sub>50</sub>Ni<sub>50</sub>/MC and

Pt<sub>100</sub>/MC catalysts at 50 mV s<sup>-1</sup> are 122.1, 110.2, 85.6, and 34.1 mA/cm<sup>2</sup>, respectively, showing that the activity of the ternary Pt<sub>50</sub>Ru<sub>40</sub>Ni<sub>10</sub>/MC catalyst is a factor of ~4 times higher than that of the Pt/MC catalyst. Almost no activity variation was observed, even after 6 h of uninterrupted cycling of the potential between 0 and 0.8 V,

Table 2. CV results of Pt<sub>50</sub>Ru<sub>40</sub>Ni<sub>10</sub>/MC, Pt<sub>50</sub>Ru<sub>50</sub>/MC, Pt<sub>50</sub>Ni<sub>50</sub>/MC and Pt<sub>100</sub>/MC electrocatalysts at room temperature

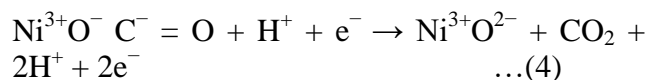
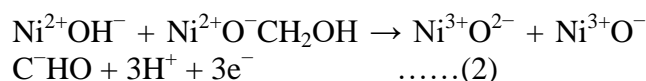
Catalyst	Scan rate 50 mV s <sup>-1</sup>	
	Positive peak potential (mV vs. Ag/AgCl)	Peak current density (mA/cm <sup>2</sup> )
Pt <sub>100</sub> /MC	797	34.1
Pt <sub>50</sub> Ni <sub>50</sub> /MC	795	85.6
Pt <sub>50</sub> Ru <sub>50</sub> /MC	779	110.2
Pt <sub>50</sub> Ru <sub>40</sub> Ni <sub>10</sub> /MC	801	122.1

The CV results show that pure Pt<sub>100</sub>/MC catalysts do not behave as an appropriate anode for MOR due to its poisoning by strongly adsorbed intermediates such as CO. However, the introduction of Ru and Ni promotes the electrocatalytic activity. The onset potentials of methanol electro oxidation for binary Pt<sub>50</sub>Ru<sub>50</sub>/MC and Pt<sub>50</sub>Ni<sub>50</sub>/MC catalysts are at about 0.4 V vs. Ag/AgCl. While for ternary Pt<sub>50</sub>Ru<sub>40</sub>Ni<sub>10</sub>/MC catalyst the onset potential for methanol electro-oxidation is earlier at about 0.3 V vs. Ag/AgCl, i.e. shifted to negative potential by 0.1 V. This observation can be explained by the more pronounced oxophilic character of Ru at low potentials in comparison with Ni.

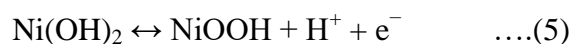
The superior activity of the Pt<sub>50</sub>Ru<sub>40</sub>Ni<sub>10</sub>/MC electrocatalyst can be attributed to the combination of electronic effect and bifunctional mechanism [15-17]. The ternary composition (Pt<sub>50</sub>Ru<sub>40</sub>Ni<sub>10</sub>/MC) presented much higher current density than the binary Pt<sub>50</sub>Ru<sub>50</sub>/MC and Pt<sub>50</sub>Ni<sub>50</sub>/MC catalysts, indicating that the activity of the ternary electrocatalysts toward MOR was much better than that of the binary compositions. It has recently been reported that nickel or nickel hydroxides acting as a catalyst not as a promoter or supporter are capable of oxidizing methanol in alkaline or acid solution. Kowal et al. investigated nickel hydroxide (NiOOH/Ni(OH)<sub>2</sub>) on the nickel metal electrode for methanol oxidation in alkaline solutions (NaOH and KOH) [18]. On the other hand, methanol oxidation in acidic solution was performed [19].

indicating the facile removal of adsorbed CO intermediates. Table 2 summarizes the CV results of Pt<sub>50</sub>Ru<sub>40</sub>Ni<sub>10</sub>/MC, Pt<sub>50</sub>Ru<sub>50</sub>/MC, Pt<sub>50</sub>Ni<sub>50</sub>/MC and Pt<sub>100</sub>/MC electrocatalysts including the positive peak potentials and the corresponding peak current densities of methanol electro-oxidation (MOR).

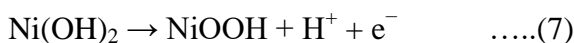
The following reaction schemes were proposed, noteworthy including nickel hydroxide as the reagent for methanol oxidation:



The reaction is completed with an attack by water on a surface carboxyl group. In addition, according to the reversible redox in reaction scheme 2, Ni(OH)<sub>2</sub> in the CH<sub>3</sub>OH/H<sub>2</sub>SO<sub>4</sub> solution can be converted to NiOOH, which is a stable phase in the catalyst:



The surface layer of the Pt–Ni or Pt–Ru–Ni contains both Ni(OH)<sub>2</sub> and NiOOH. The mixed-valence Ni<sup>3+/2+</sup> components account for the high electronic conductivity of the surface layer, are relatively stable in acidic media, and have a confirmed catalytic activity. The Ni hydroxide layer has some other favorable properties, such as proton and electronic conductivity, and is well protected from corrosion under methanol oxidation conditions. Such a hydroxide layer on the Pt–Ni and Pt–Ru–Ni may display high catalytic activity with respect to methanol oxidation. Therefore, we propose the following reaction scheme for Pt–Ni nanoparticles:



### Chronoamperometry

Fig. 5 shows the current densities measured at a constant potential jumping from 0.1 to 0.8 V in 1.0 M methanol+0.5 M H<sub>2</sub>SO<sub>4</sub> at room temperature. The currents decay with time in a parabolic style and reach an apparent steady state within 80s. It can be seen that the current density of methanol electro-oxidation on the Pt<sub>50</sub>Ru<sub>40</sub>Ni<sub>10</sub>/MC catalyst is higher than that on the Pt<sub>50</sub>Ru<sub>50</sub>/MC, Pt<sub>50</sub>Ni<sub>50</sub>/MC, Pt<sub>100</sub>/MC catalyst at the same potentials. The activity change for methanol oxidation decreases in the order of Pt<sub>50</sub>Ru<sub>40</sub>Ni<sub>10</sub>/MC > Pt<sub>50</sub>Ru<sub>50</sub>/MC > Pt<sub>50</sub>Ni<sub>50</sub>/MC > Pt<sub>100</sub>/MC, which is in fairly good agreement with our CV results.

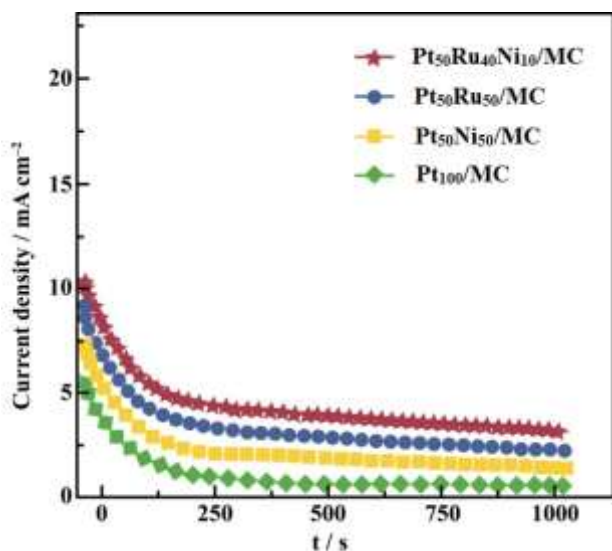


Fig. 5. Chronoamperometry of Pt<sub>50</sub>Ru<sub>40</sub>Ni<sub>10</sub>/MC, Pt<sub>50</sub>Ru<sub>50</sub>/MC, Pt<sub>50</sub>Ni<sub>50</sub>/MC and Pt<sub>100</sub>/MC electrocatalysts at room temperature

For the durability test, the CA experiments were carried out at 0.1 to 0.8 V for 1000 s in the same conditions. Before each measurement, the solution was purged with high-purity nitrogen gas for at least 30 min to ensure oxygen-free measurements.

### Single Cell Performance

The microfluidic architecture of laminar flow-based membraneless fuel cells overcomes the fuel crossover and water management issues that plague membrane-based fuel cells (i.e., PEMFC, DMFC) and enables independent control of stream characteristics (i.e., flow-rate and composition). Here we focused on

maximizing cell performance, in terms of power density, by tailoring various structural characteristics and catalytic activity of mesoporous carbon supported ternary Pt–Ru–Ni catalysts. A single cell performance was tested using Pt<sub>50</sub>Ru<sub>40</sub>Ni<sub>10</sub>/MC, Pt<sub>50</sub>Ru<sub>50</sub>/MC, Pt<sub>50</sub>Ni<sub>50</sub>/MC and Pt<sub>100</sub>/MC electrocatalysts as the anode. Polarization curves and power densities at room temperature are shown in Fig. 6. The catalyst loadings are 2 mg cm<sup>-2</sup> at both electrodes and Pt<sub>100</sub>/MC was used as the cathode catalyst.

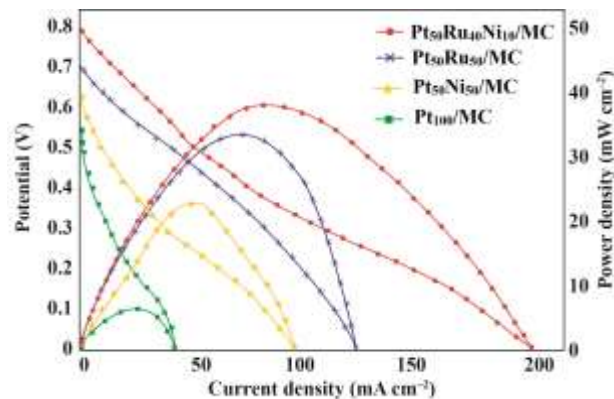


Fig. 6. Polarization and power density curves of different catalyst at 2 mg cm<sup>-2</sup> catalyst loading on anode and cathode at room temperature

For each catalyst, the open-circuit voltages (OCV) were different, as would be expected in onset potentials. The OCVs of Pt<sub>50</sub>Ru<sub>40</sub>Ni<sub>10</sub>/MC, Pt<sub>50</sub>Ru<sub>50</sub>/MC and Pt<sub>50</sub>Ni<sub>50</sub>/MC are higher than that of Pt<sub>100</sub>/MC, 0.53 V, and the order of OCV is exactly same as the onset potentials. The OCV of Pt<sub>50</sub>Ru<sub>40</sub>Ni<sub>10</sub>/MC is the highest value of 0.80 V, which is approximately 0.26 V higher than that of Pt<sub>100</sub>/MC. It indicates that Pt<sub>100</sub>/MC is more rapidly poisoned by CO than any other alloy catalyst and that the oxidation of adsorbed CO is enhanced by the second or third metal. In the case of Pt<sub>50</sub>Ru<sub>40</sub>Ni<sub>10</sub>/MC the overall performance is superior to that of the bimetallic electrocatalysts. Although the difference between Pt<sub>50</sub>Ru<sub>50</sub>/MC and Pt<sub>50</sub>Ru<sub>40</sub>Ni<sub>10</sub>/MC is relatively small in the low-current-density region, the alloying effect of Ni becomes larger as the current density increases. The maximum power densities obtained for Pt<sub>50</sub>Ru<sub>40</sub>Ni<sub>10</sub>/MC, Pt<sub>50</sub>Ru<sub>50</sub>/MC and Pt<sub>50</sub>Ni<sub>50</sub>/MC are 38.1, 33.2, and 23.3 mW cm<sup>-2</sup>, respectively (Table 3). We conclude that the substitution of a small amount of Ni for Ru aids in cleaning surfaces poisoned by CO and provides additional reaction sites for methanol oxidation.

Table 3. Summary of performance of single fuel cell tests

Anode catalysts	Open circuit Voltage (V)	Maximum power density (mW cm <sup>-2</sup> )	Maximum current density (mA cm <sup>-2</sup> )
Pt <sub>100</sub> /MC	0.53	6.7	48.4
Pt <sub>50</sub> Ni <sub>50</sub> /MC	0.63	23.3	100.2
Pt <sub>50</sub> Ru <sub>50</sub> /MC	0.71	33.2	130.1
Pt <sub>50</sub> Ru <sub>40</sub> Ni <sub>10</sub> /MC	0.80	38.1	199.0

In membraneless fuel cells, pure Pt/MC catalyst does not behave as a very good anode for methanol electro-oxidation due to its poisoning by strongly adsorbed intermediates such as CO. The binary and ternary electrocatalysts performed better than Pt/MC for methanol oxidation. Moreover, when the binary electrocatalysts were compared to the ternary ones in terms of oxidation the latter catalysts gave the best electrical performances. On the other hand, addition of Ni to Pt (Pt–Ni/MC) had a little effect, whereas addition of Ni to Pt–Ru/MC greatly enhanced the electrocatalytic activity. The best performance observed for these electrocatalysts could be explained by a bifunctional mechanism and ligand (electronic) effect, as well assumed for various Pt-based electrocatalysts.

As mentioned in our earlier studies, the effects of percarbonate concentration on the cell performance were investigated at different concentrations and the power density increased as sodium percarbonate concentration increases in the membraneless fuel cell system. The results demonstrated that the performance of the developed membraneless fuel cell enhanced profoundly if the concentration of oxidant in cathodic stream is 10 times larger, and the current density is also increased approximately ten times.

Microfluidic membraneless fuel cells avoid many of the issues associated with polymer electrolyte membrane-based fuel cells such as humidification, membrane degradation, water management, and fuel crossover. Moreover, miniaturization of membraneless fuel cells has drawn significant interest because of potential advantages: compact design, high-energy conversion efficiency, low operating temperature, environmental-friendly emissions, use of both metallic and biological catalysts and elimination of moving parts, hence we expect MLMFC would be better than polymer electrolyte membrane-based fuel cells.

## Conclusions

In the present work, the study of methanol oxidation on carbon-supported Pt–Ru–Ni ternary nanoparticles has revealed details concerning the activity and stability of the catalysts in membraneless fuel cells. The maximum activity for methanol oxidation was found for the Pt<sub>50</sub>Ru<sub>40</sub>Ni<sub>10</sub>/MC than the Pt<sub>50</sub>Ru<sub>50</sub>/MC, Pt<sub>50</sub>Ni<sub>50</sub>/MC and Pt<sub>100</sub>/MC. The significantly enhanced catalytic activity for methanol oxidation can be attributed to the high dispersion of ternary catalysts and to Ni acting as a promotion agent. XRD results show the homogenous alloy structure of Pt, Ru and Ni. The TEM images indicated an average size of Pt<sub>50</sub>Ru<sub>40</sub>Ni<sub>10</sub>/MC nanoparticle of 3–5 nm with a narrow size distribution. The atom ratio of Pt, Ru and Ni from EDX analyses is close agreement with the original precursor concentration. The composition of ternary Pt<sub>50</sub>Ru<sub>40</sub>Ni<sub>10</sub>/MC nanoparticles can be conveniently controlled by adjusting the initial metal salt solution and preparation conditions. The electrochemical experiments showed that the mesoporous carbon-supported Pt–Ru–Ni nanoparticles have higher catalytic activity toward methanol oxidation at room temperature than that of the bimetallic catalysts. We expect that the MLMFC may be a promising candidate for practical fuel cells to establish a clean and sustainable energy future. Further work is necessary to characterize the catalysts using different surface analysis techniques and to conduct tests of these electrocatalysts in microfluidic membraneless fuel cells.

## Conflict of interest

Authors declare there are no conflicts of interest.

## References

- [1] Vijayaramalingam K, Kiruthika S and Muthukumaran B. Promoting Effect of Third Metal (M = Ni, Mo and Rh) on Pd–Ir Binary Alloy Catalysts in Membraneless Sodium Perborate Fuel Cells. *International*

- Journal of Modern Science and Technology. 2016; 3(7):257–263.
- [2] Kalaikathir SPR, Begila David S. Synthesis and characterization of nanostructured carbon-supported Pt electrocatalysts for membraneless methanol fuel cells. *International Journal of Modern Science and Technology*. 2016;1(6):199–212
- [3] Biegler T, Rand DAJ and Woods R, Limiting oxygen coverage on platinumized platinum; Relevance to determination of real platinum area by hydrogen adsorption. *Journal of Electroanalytical Chemistry*. 1971;29(2):269-277.
- [4] Bonesi A, Moreno MS, Triaca WE and Castro Luna AM. Modified catalytic materials for ethanol oxidation. *International Journal of Hydrogen Energy*. 2010;35(11):5999-6004.
- [5] Cao J, Du C, Wang SC, Mercier P, Zhang X, Yang H. The production of a high loading of almost monodispersed Pt nanoparticles on single-walled carbon nanotubes for methanol oxidation. *Electrochem. Commun.* 2007;9(4):735–740.
- [6] Liu H, Song C, Zhang L, Zhang J, Wang H, Wilkinson DP. A review of anode catalysis in the direct methanol fuel cell. *J. Power Sources*. 2006;155(2):95-102.
- [7] Mukerjee S, Lee SJ, Ticcianelli E, McBreen J, Grur BN, Markovic NM. Investigation of enhanced CO tolerance in proton exchange membrane fuel cells by carbon supported PtMo alloy catalyst. *Electrochem. Solid State Lett.* 1999;2(1):12-19.
- [8] Neto AO, Franco EG, Arico E, Linardi M, Gonzalez ER, Electro-oxidation of methanol and ethanol on Pt-Ru/C and Pt-Ru-Mo/C electrocatalyst prepared by bonnemann's method. *J. of the European Ceramic Society*. 2003; 23(15): 2987-2992.
- [9] Oetjen HF, Schmidt VM, Stimming U, Trila F. Performance data of a proton exchange membrane fuel cell using H<sub>2</sub>/CO as fuel gas. *J Electrochem. Soc.* 1996;143: 3838-3842.
- [10] Gotz M, Wendt H. Binary and ternary anode catalyst formulations including the elements W, Sn and Mo for PEMFCs operated on methanol or reformat gas. *Electrochimica Acta*. 1998;43(24):3637-3644.
- [11] Beyhan S, Leger J-M, Kadırgan F. Pronounced synergetic effect of the nano-sized PtSnNi/C catalyst for methanol oxidation in direct methanol fuel cell. *Applied Catalysis B: Environmental*. 2013;130:305–313.
- [12] Radmilovic V, Gasteiger HA, Ross Jr. PN. Structure and chemical composition of a supported Pt-Ru electrocatalyst for methanol oxidation. *J Catal.* 1995;154(1):98-106.
- [13] Rashidi R, Dincer I, Naterer GF, Berg P. Performance evaluation of direct methanol fuel cells for portable applications. *J. Power Sources*. 2009;187(2):509-515.
- [14] Zhou Z, Wang S, Zhou W, Wang G, Jiang L, Li W. Pt based anode catalysts for direct ethanol fuel cell. *Chem. Commun.* 2003;46(4):394–395.
- [15] Watanabe M, Motoo S. Electrocatalysis by ad-atoms: Part XXIII, Design of platinum ad-electrodes for formic acid fuel cells with ad-atoms of the IVth and the Vth groups. *J Electroanal Chem.* 1988;250(1):117–125.
- [16] Cooper JS, McGinn PJ. Combinatorial screening of thin film electrocatalysts for a direct methanol fuel cell anode. *J Power Sources*. 2006;163(1):330–338.
- [17] Choi SM, Kim JH, Jung JY, Yoon EY, Kim WB. Pt nanowires prepared via a polymer template method: Its promise toward high Pt-loaded electrocatalysts for methanol oxidation. *Electrochimica Acta*. 2008;53(19):5804–5811.
- [18] Priya M, Elumalai M, Kiruthika S and Muthukumar B. Influences of supporting materials for Pt-Ru binary catalyst in Ethanol fuel cell, *International Journal of Modern Science and Technology*. 2016;1(1):5–11.
- [19] Mahendran S, Anbuselvan C. Kinetics and mechanism of oxidation of 5-(4'-bromophenyl)-5-oxopentanoic acid by acid permanganate. *International Journal of Modern Science and Technology*. 2016;3(1):106–110.

\*\*\*\*\*